NOAA-15 HIRS/3 AND AMSU TRANSMITTANCE MODEL VALIDATION

Harold Woolf, Paul van Delst and Wenjian Zhang*

Cooperative Institute for Meteorological Satellite Studies
University of Wisconsin-Madison
Madison WI, USA

***National Satellite Meteorological Center**
Beijing, People's Republic of China

1. INTRODUCTION

An essential part of a satellite sounding system is the accuracy of the fast forward transmittance model used to simulate instrument observations. Advances in both satellite instrumentation and Numerical Weather Prediction (NWP) must be accompanied by similar improvements in the parameterization of radiative transfer through the atmosphere. This paper examines initial results of the AMSU/HIRS regression transmittance model based on the Pressure Layer Optical Depth (PLOD) algorithm developed for the EOS-PM1 AIRS instrument by *Hannon et al* (1996) and implemented at CIMSS for the AMSU/HIRS instruments. Comparisons are made between regression and line-by-line monochromatic transmittance calculations as well as AMSU/HIRS observations.

2. MONOCHROMATIC TRANSMITTANCE DATABASE CALCULATIONS

2.1 Dependent profile set

The number of dependent set atmospheres used to generate the monochromatic transmittance database was 32. These 32 atmospheric profiles are the "standard" set used previously in generation of transmittances for earlier versions of RTTOV (e.g. *Eyre*, 1991) and OPTRAN, chosen to represent the full range of global atmospheric conditions. The minimum and maximum temperature, water vapor, and ozone profiles as well as the column precipitable water for each of the dependent set profiles are shown in figure 1.

2.2 Infrared transmittance calculations

For the infrared spectral region, the transmittances were calculated using LBLRTM (*Clough and Iacono*, 1995) and HITRAN96 at five local zenith angles, θ, from 0 to 60°. The absorbing constituents were separated into four groups: water vapor line, water vapor continuum, ozone, and the "fixed" or "dry" gases, i.e. everything except water vapor and ozone. The total transmittance is determined by multiplying the four components together:

$$\tau_{total} = \tau_{fixed} \cdot \tau_{ozone} \cdot \tau_{wet} \cdot \tau_{continuum} \qquad (1)$$

where τ_{wet} is the contribution of water vapor lines only and $\tau_{continuum}$ is the contribution of the water vapor continuum only. To ensure that the product rule is not violated, the fixed gas and ozone transmittances in eqn. 1 are determined using

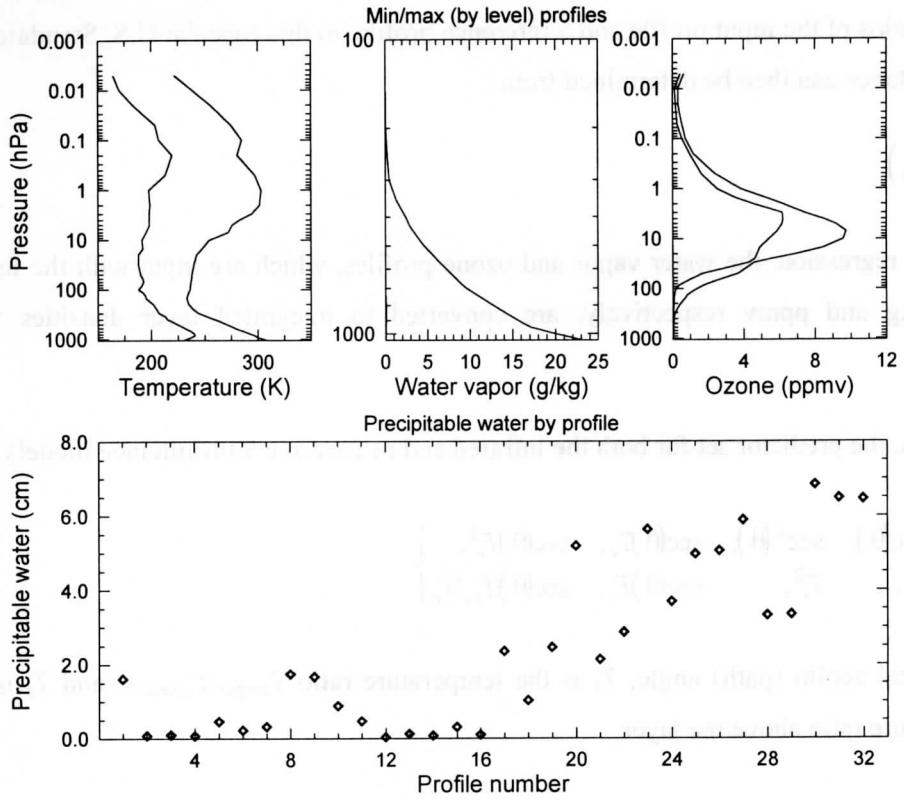

Figure 1. (*Top*) Minimum and maximum temperature, water vapor (minimum close to zero throughout column), and ozone profiles for the **dependent** profile set. (*Bottom*) Precipitable water amount for each profile.

$$\tau_{ozone} = \tau_{wvo} / \left(\tau_{wet} \cdot \tau_{continuum} \right) \text{, and} \tag{2a}$$

$$\tau_{fixed} = \tau_{all} / \tau_{wvo} \tag{2b}$$

where τ_{wvo} is the transmittance due to water vapor lines plus continuum and ozone lines, and τ_{all} is the transmittance due to all molecules and water vapor continuum. This guarantees that τ_{total}, the product of eqn. 1, is the same as τ_{all}.

2.3 Microwave transmittance calculations

For the microwave spectral region, code developed at CIMSS based on the work of *Rosenkranz* (1975) and *Barrett and Chung* (1962) is used. The microwave calculations are performed differently from those for the infrared, in that the oxygen and water vapor transmittances are calculated separately and simply multiplied together to provide the total transmittance.

3. REGRESSION MODEL METHODOLOGY

The optical depth, σ, of an atmospheric layer, j, for a particular channel is determined using,

$$\sigma_j = a_{j0} + \sum_{k=1}^{K} a_{jk} \cdot X_{kj} \tag{3}$$

where a is the matrix of regression coefficients and X is the matrix of predictors, which primarily consist of combinations of ratios of the input profile and a reference profile, in this case the U.S. Standard Atmosphere. The layer transmittance can then be determined from

$$\tau_j = \ln(-\sigma_j) \tag{4}$$

Prior to the actual regression, the water vapor and ozone profiles, which are input with the familiar mixing ratio units of g/kg and ppmv respectively, are converted to integrated layer densities with units of k.mole/cm^2.

For the fixed gases, the predictor set for both the infrared and microwave transmittance models is

$$X_{fixed} = \begin{Bmatrix} \sec(\theta), & \sec^2(\theta), & \sec(\theta)T_r, & \sec(\theta)T_r^2, \\ T_r, & T_r^2, & \sec(\theta)T_z, & \sec(\theta)T_z/T_r \end{Bmatrix} \tag{5}$$

where θ is the local zenith (path) angle, T_r is the temperature ratio $T_{profile}/T_{reference}$, and T_z is the pressure weighted temperature ratio above the layer,

$$T_z(j) = \sum_{i=2}^{j} P(i)\Delta P(i)T_r(i-1) \tag{6}$$

with $P(i)$ being the average pressure for layer i.

For water vapor, the calculation is performed in two parts: one case where the total water optical depth above the current layer is less than or equal to a threshold value, $\sigma_{wet\_threshold}$, and another where the total water optical depth is greater than the threshold. Currently the total water optical depth threshold is 3.0. The water vapor predictor set is

$$X_{wet}(\sigma \le \sigma_{wet\_threshold}) = \begin{Bmatrix} \sec(\theta)W_r, & \sqrt{\sec(\theta)W_r}, & \sec(\theta)W_r\Delta T, & (\sec(\theta)W_r)^2, \\ \sec(\theta)W_r\Delta T|\Delta T|, & (\sec(\theta)W_r)^3, & \sec(\theta)W_z, & \sqrt{\sec(\theta)W_r}\Delta T, \\ \sqrt[4]{\sec(\theta)W}, & (\sec(\theta)W_z)^2, & \sqrt{\sec(\theta)W_r} & \end{Bmatrix}$$
$$X_{wet}(\sigma > \sigma_{wet\_threshold}) = \begin{Bmatrix} \sec(\theta)W_r, & \sqrt{\sec(\theta)W_r} \end{Bmatrix} \tag{7}$$

where W_r is the water amount ratio, $W_{profile}/W_{reference}$, ΔT is the temperature offset from the reference atmosphere, $T_{profile}$-$T_{reference}$, and W_z is the pressure weighted water amount ratio above the layer,

$$W_z(j) = \frac{\sum_{i=1}^{j} P(i)\Delta P(i)W_{profile}(i)}{\sum_{i=1}^{j} P(i)\Delta P(i)W_{reference}(i)} \tag{8}$$

The use of different predictor sets based on total water optical depth is intended to take into account abrupt changes in the dependence of the water vapor predictors at optical depths of 3-5 (*Hannon et al.*, 1996). Note that only the first set of water vapor predictors, where $\sigma \leq \sigma_{wet\_threshold}$, is used for the microwave transmittance model.

The ozone predictors used in the infrared transmittance model are,

$$X_{ozone} = \begin{Bmatrix} \sec(\theta)O_r, & \sqrt{\sec(\theta)O_r}, & \sec(\theta)O_r\Delta T, & (\sec(\theta)O_r)^2, \\ \sqrt{\sec(\theta)O_r}\Delta T, & \sec(\theta)O_z, & \sec(\theta)O_r\sqrt{\sec(\theta)O_z}, & \sec^2(\theta)O_rW_r, \\ \sec(\theta)O_rTO_z & & & \end{Bmatrix} \quad (9)$$

where O_r is the ozone amount ratio, $O_{profile}/O_{reference}$, O_z is the pressure weighted ozone amount ratio above the layer,

$$O_z(j) = \sum_{i=2}^{j} P(i)\Delta P(i)O_r(i-1) \quad (10)$$

and TO_z is the pressure and ozone weighted temperature ratio above the layer,

$$TO_z(j) = \sum_{i=2}^{j} P(i)\Delta P(i)T_r(i-1)O_r(i-1) \quad (11)$$

Finally, the water vapor continuum predictors used in the infrared transmittance model are

$$X_{continuum} = \{\sec(\theta)W_rT_r^2, \quad \sec(\theta)W_r^2T_r^4, \quad \sec(\theta)W_r/T_r, \quad \sec(\theta)W_r^2/T_r \quad (12)$$

The AIRS PLOD methodology as described in *Hannon et al.* (1996) applies a weighting factor to the transmittances before performing the regression. This is done to weight the contribution of a particular layer's transmittance in the regression according to its impact on radiative transfer accuracy. Currently this weighting is not performed in the CIMSS PLOD implementation.

4. REGRESSION AND LINE-BY-LINE COMPARISONS

4.1 Dependent profile set

The dependent profile set regression minus line-by-line statistics for the AMSU and HIRS transmittance models are shown in figures 2 and 3 respectively. Despite the fact that one expects the dependent set residuals to be small, the AMSU RMS residuals are very good, in most cases an order of magnitude below the temperature sensitivity of the instrument. Even the maximum AMSU brightness temperature residuals are less than the expected sensitivities. The performance of the HIRS PLOD model using the dependent profile set is not as impressive as that for AMSU with the HIRS RMS residuals for the long- and midwave channels

(1-12) at about the same level as the specified instrument sensitivity. The shortwave channel (13-19) residual magnitudes are similar to the longwave but greater than expected instrument noise.

The poorer performance of the HIRS water vapor channel 11 could be due to the fact that the CIMSS PLOD model does not weight the layer optical depths as described previously. Since the change in transmittance across layers is small for the middle to upper regions of the troposphere in the water vapor channels, this weighting could improve the residuals for the less opaque channel 11.

4.2 Independent profile set

The independent set used in this comparison was a small set of 16 atmospheres constructed from climatology and radiosonde profiles for each of the standard model atmospheres – tropical through subarctic winter. The minimum and maximum temperature, water vapor, and ozone profiles as well as the column precipitable water for the independent set profiles are shown in figure 4. The independent set used is admittedly small and will be expanded for future analysis.

The independent profile set transmittance model residuals for the AMSU and HIRS are shown in figures 5 and 6 respectively. Performance of both the AMSU and HIRS transmittance models is similar to that for the dependent set, with RMS residuals at approximately the same level. The greatest changes were in the HIRS channel 9 and channels 13-16 where the RMS residuals increased by factors of 2-4. The increase for HIRS channel 9 is not unexpected when one compares the minimum/maximum profiles of the dependent and

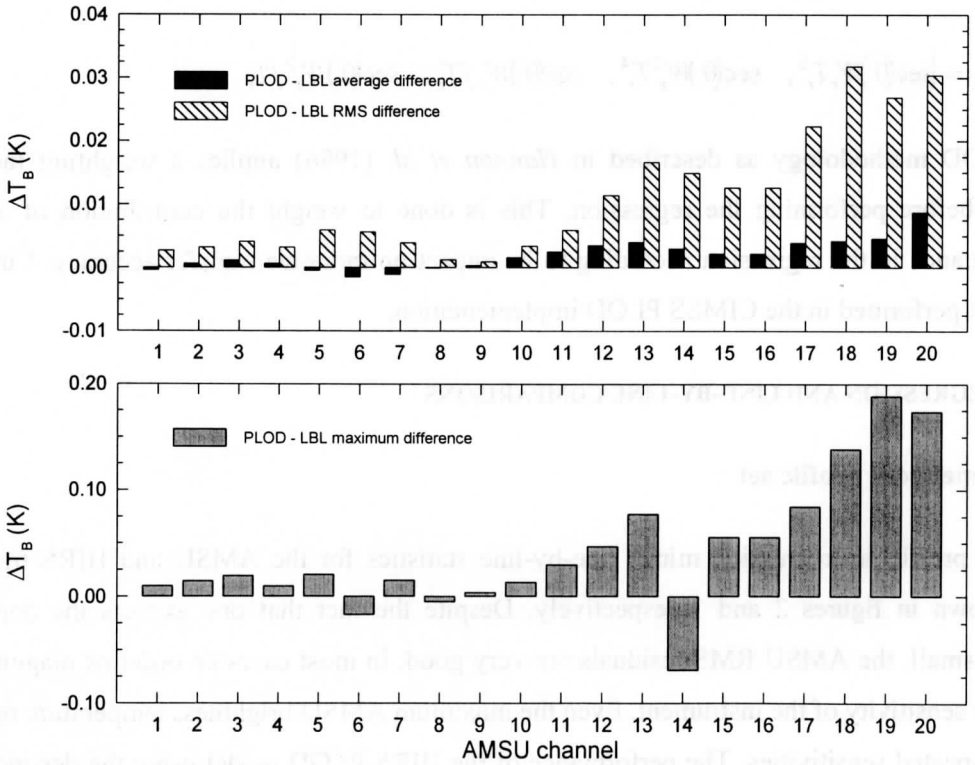

Figure 2. AMSU brightness temperature residuals between the PLOD regression fast model and microwave LBL model for the **dependent** profile set. (*Top*) Average and RMS residual. (*Bottom*) Maximum residual.

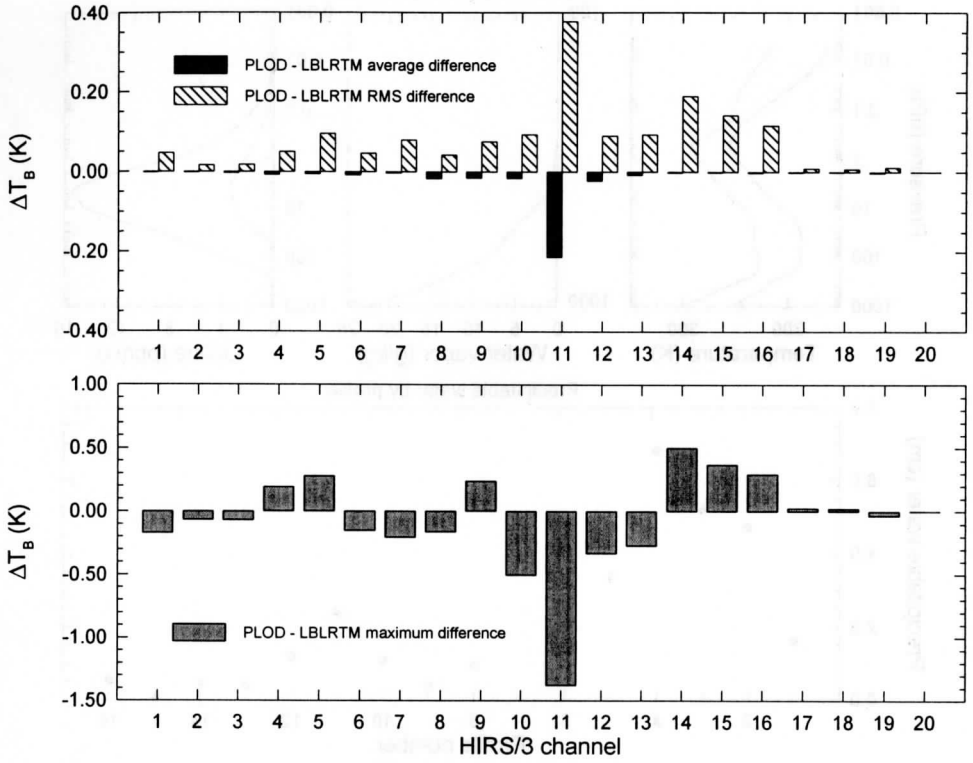

Figure 3. HIRS/3 brightness temperature residuals between the PLOD regression fast model and LBLRTM for the **dependent** profile set. (*Top*) Average and RMS residual. (*Bottom*) Maximum residual.

independent sets (see figures 1 and 4), with the range of ozone profile values in the latter being much larger.

5. RADIANCE BIAS CALCULATION

Physical retrieval schemes for retrieving meteorological parameters from NOAA-15 HIRS and AMSU measurements require the removal of systematic errors, or biases, which arise from uncertainties in both the forward model algorithm and the measurements (e.g. radiance calibration). A successful retrieval product is dependent to a great degree on how well the calculated radiances or brightness temperatures have been corrected.

To assess the accuracy of the PLOD forward model with observations, a "truth" data set was established by matching global radiosonde measurements with HIRS/AMSU measurements. The criteria used in constructing the match-up data set were as follows:

- The match sample is based upon the ATOVS retrieval footprint (3×3 HIRS field-of-view (FOV) array for our retrieval algorithm) and the nearest temporally and spatially co-located radiosonde observation. The central FOV position is used to represent the location of the measurements.
- The distance between the sonde launch site and the central FOV of the measurements must be less than 1.0°.
- The time difference between the radiosonde and the HIRS/AMSU measurements must be less than 2 hours.

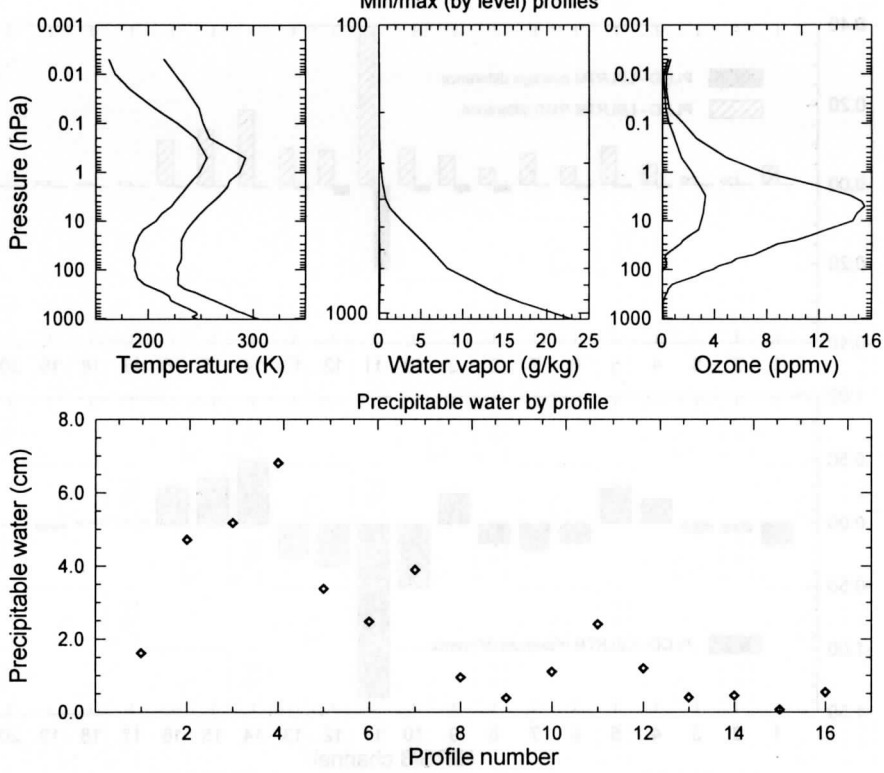

Figure 4. (*Top*) Minimum and maximum temperature, water vapor (minimum close to zero throughout column), and ozone profiles for the **independent** profile set. (*Bottom*) Precipitable water amount for each profile.

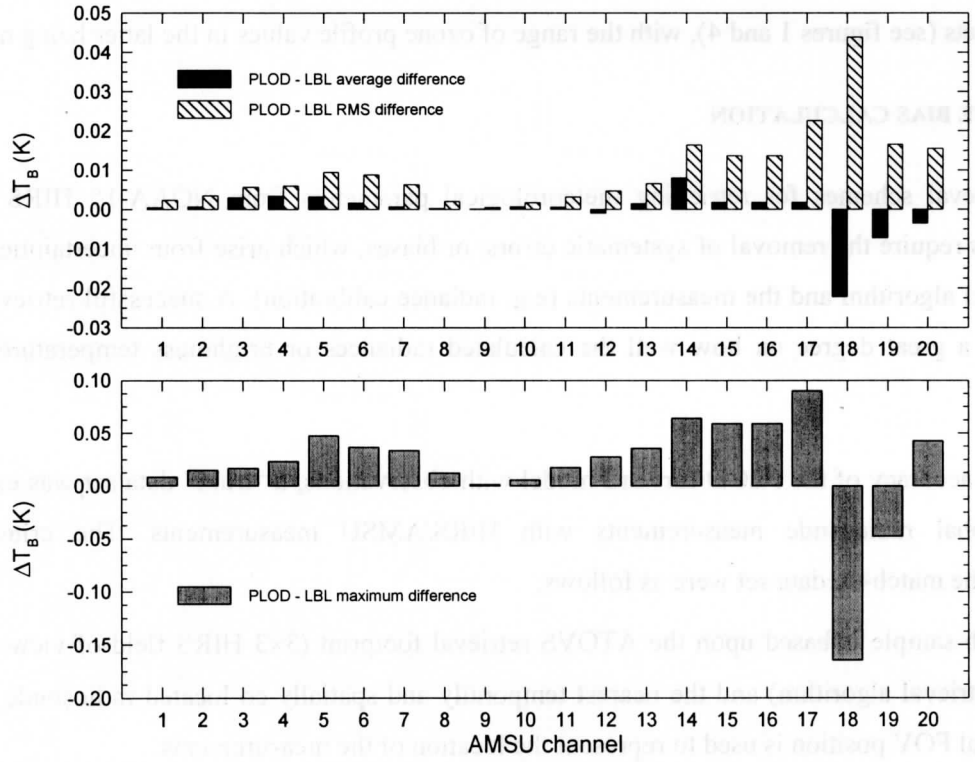

Figure 5. AMSU brightness temperature residuals between the PLOD regression fast model and microwave LBL model for the **independent** profile set. (*Top*) Average and RMS residual. (*Bottom*) Maximum residual.

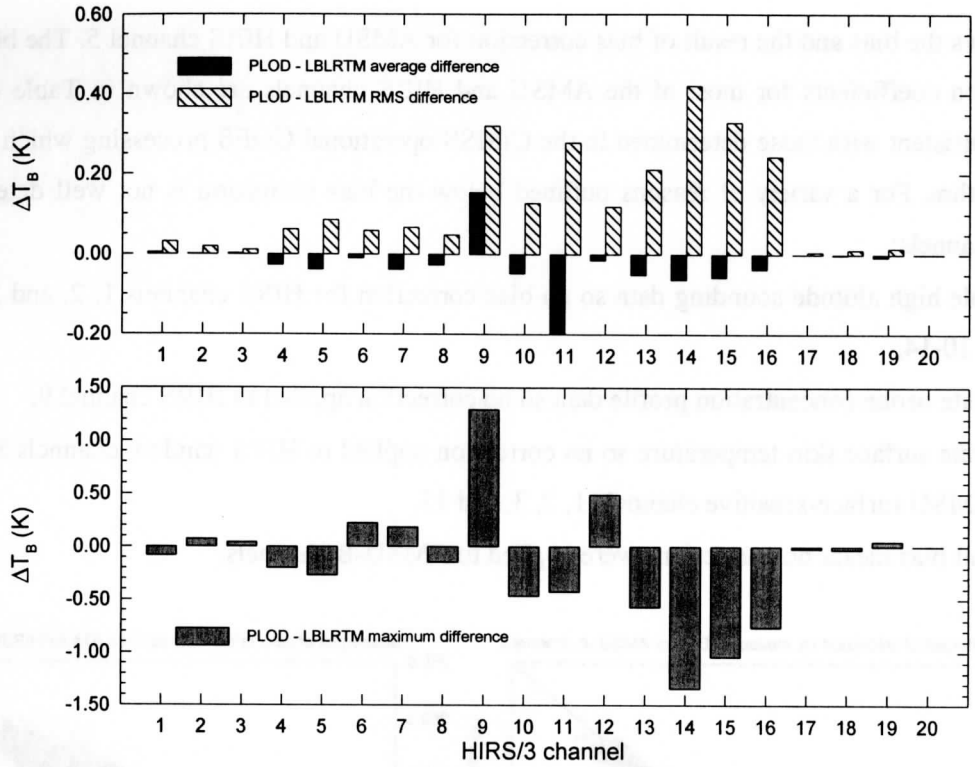

Figure 6. HIRS/3 brightness temperature residuals between the PLOD regression fast model and LBLRTM for the **independent** profile set. (*Top*) Average and RMS residual. (*Bottom*) Maximum residual.

- The zenith angle of the satellite measurements must be less than 25°.
- Only radiosondes whose sounding height is above 100mb were selected.

For the period of November 4-17, 1998, the above criteria gave a total of 5011 matched samples from 33 orbits.

The matched cases were then screened for cloud contamination. The method used was to check the measurements for both channel coherence (consistency of different channel measurements for the same instrument) and spatial coherence (consistency between HIRS and AMSU measurements). The HIRS measurements were used to determine an initial cloud check. Only the subsequent clear cases were then checked for cloudiness using the AMSU measurements. After removing the cloudy samples, 1522 match ups remained.

For each co-located sample, the channel brightness temperatures were calculated using the CIMSS PLOD algorithm. A linear regression relationship between the measured and calculated brightness temperatures was next determined for each channel. The calculated regression coefficients were then used to apply the bias correction,

$$\begin{aligned} HIRS_{corrected}(i) &= [a_{HIRS}(i) \cdot HIRS_{observed}(i)] + b_{HIRS}(i) \quad i = 1,2,...,19 \\ AMSU_{corrected}(i) &= [a_{AMSU}(i) \cdot AMSU_{observed}(i)] + b_{AMSU}(i) \quad i = 1,2,...,20 \end{aligned} \tag{13}$$

Figure 7 shows the bias and the result of bias correction for AMSU and HIRS channel 5. The bias correction and correlation coefficients for most of the AMSU and HIRS channels are shown in Table 1. The HIRS biases are consistent with those determined in the CIMSS operational GOES processing which also uses the PLOD algorithm. For a variety of reasons outlined below the bias correction is not well determined for a number of channels:

- No reliable high altitude sounding data so no bias correction for HIRS channels 1, 2, and 3 and AMSU channels 10-14,
- No accurate ozone concentration profile data so no correction applied to HIRS channel 9,
- No accurate surface skin temperature so no correction applied to HIRS window channels 8, 13, 18, and 19 and AMSU surface-sensitive channels 1, 2, 3, and 15,
- Instrument bias meant no corrections were applied to AMSU-B channels.

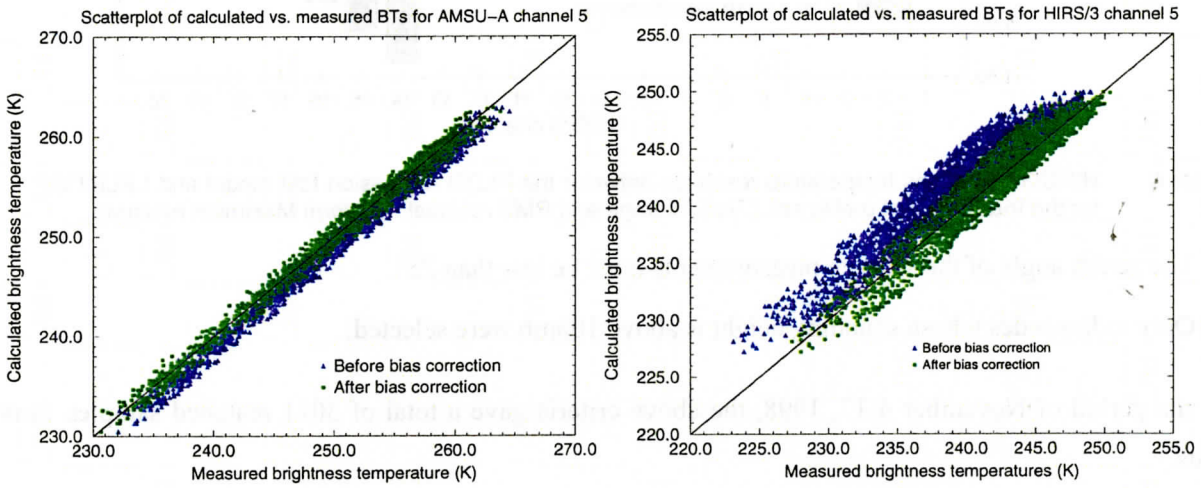

Figure 7. Scatterplot of (*Left*) AMSU-A channel 5 and (*Right*) HIRS/3 channel 5 calculated vs. measured brightness temperatures before and after bias correction.

6. CONCLUSIONS AND FURTHER WORK

The implementation of the PLOD algorithm has led to an improvement in forward model accuracy over previous algorithms used at CIMSS. One development that would lead to model improvement, if only by consensus, is co-ordination with the TOVS community in the assembling of the dependent and independent profile data sets used to generate and test the regression coefficients. Implementation of code to determine analytic Jacobians is also planned. The impact of this and the bias correction on HIRS/AMSU retrievals, as well as updates to the line-by-line microwave transmittance calculations, are the next avenues of investigation.

7. ACKNOWLEDGMENTS

This work was funded under NOAA Grant NA67EC0100.

AMSU channel	a_{AMSU}	b_{AMSU}	r_{AMSU}	HIRS channel	a_{HIRS}	b_{HIRS}	r_{HIRS}
4	1.020	7.771	0.969	4	1.208	5.484	0.979
5	1.022	6.488	0.995	5	0.988	3.673	0.994
6	1.008	1.507	0.994	6	0.975	6.597	0.992
7	1.039	8.766	0.979	7	0.958	10.525	0.982
8	0.938	13.425	0.960	8	-	-	-
9	0.942	12.654	0.980	9	-	-	-
10	-	-	-	10	0.933	18.650	0.958
11	-	-	-	11	0.898	25.740	0.946
12	-	-	-	12	0.924	18.964	0.804
13	-	-	-	13	-	-	-
14	-	-	-	14	0.985	3.132	0.990
15	-	-	-	15	0.984	2.048	0.993
16	-	-	-	16	0.992	0.152	0.994
17	-	-	-	17	0.958	11.428	0.969

Table 1. Slope and intercept bias correction and correlation coefficients for some AMSU and HIRS channels determined from the match-up dataset.

8. REFERENCES

Barrett, A.H. and V.K. Chung, 1962. High-altitude water vapor abundance from ground-based microwave observations. *Journal of Geophysical Research*, **67**, pp4259-4266

Clough, S.A. and M.J. Iacono, 1995. Line-by-line calculations of atmospheric fluxes and cooling rates. 2: Applications to carbon dioxide, ozone, methane, nitrous oxide and the halocarbons. *Journal of Geophysical Research*, **100**, pp16519-16535

Eyre, J.R., 1991. A fast radiative transfer model for satellite sounding systems. ECMWF Technical Memorandum No. 176

Hannon, S., L.L. Strow, and W.W. McMillan, 1996. Atmospheric infrared fast transmittance models: A comparison of two approaches. *Proceedings of SPIE*, **2830**, pp94-105.

Rosenkranz, P.W., 1975. Shape of the 5mm oxygen band in the atmosphere. IEEE Transactions of Antennas and Propogation, **AP-23**, pp498-506

TECHNICAL PROCEEDINGS OF THE TENTH INTERNATIONAL ATOVS STUDY CONFERENCE

Boulder, Colorado

27 January - 2 February 1999

Edited by

J. Le Marshall and J.D. Jasper

Bureau of Meteorology Research Centre, Melbourne, Australia

Published by

Bureau of Meteorology Research Centre

PO Box 1289K, GPO Melbourne, Vic., 3001, Australia

December 1999